UNIVERSITYOF BIRMINGHAM

Fractal analysis

Wang, Jie; Li, Yuancheng; Yang, Fuyao; Bravo, Laura; Wan, Ke; Xu, Yuanwei; Cheng, Wei; Sun, Jiayu; Zhu, Yanjie; Zhu, Tingxi; Gkoutos, Georgios V; Han, Yuchi; Chen, Yucheng

Link to publication on Research at Birmingham portal

Radiology

Fractal Analysis: Prognostic Value of Left Ventricular Trabecular Complexity Cardiovascular MRI in Participants with Hypertrophic Cardiomyopathy

Jie Wang, MD • Yuancheng Li, BMSci • Fuyao Yang, BMSci • Laura Bravo, PhD • Ke Wan, MD •
Yuanwei Xu, BMSci • Wei Cheng, BMSci • Jiayu Sun, MD • Yanjie Zhu, PhD • Tingxi Zhu, MPH •
Georgios V. Gkoutos, PhD • Yuchi Han, MD, MMSc • Yucheng Chen, MD

From the Department of Cardiology (J.W., Y.L., F.Y., Y.X., Y.C.), Department of Radiology (W.C., J.S., Y.C.), Department of Geriatrics (K.W.), Center of Rare Diseases (Y.C.), and Medical Big Data Center (T.Z.), West China Hospital, Sichuan University, Guoxue Xiang No. 37, Chengdu, Sichuan 610041, China; Paul C. Lauterbur Research Centre for Biomedical Imaging, Shenzhen Institutes of Advanced Technology, Chinese Academy of Sciences, Shenzhen, P. R. China (Y.Z.); College of Medical and Dental Sciences, Institute of Cancer and Genomic Sciences, University of Birmingham, Birmingham, England (J.W., L.B., G.V.G.); Medical Research Council Health Data Research, Midlands Site, Birmingham, England (G.V.G.); and Department of Medicine (Cardiovascular Division), University of Pennsylvania, Philadelphia, Pa (Y.H.). Received May 20, 2020; revision requested July 6; revision received August 13; accepted August 24. **Address correspondence to** Y.C. (e-mail: *chenyucheng2003@126.com*).

Background: The prognostic value of myocardial trabecular complexity in patients with hypertrophic cardiomyopathy (HCM) is unknown.

Purpose: To explore the prognostic value of myocardial trabecular complexity using fractal analysis in participants with HCM.

Materials and Methods: The authors prospectively enrolled participants with HCM who underwent 3.0-T cardiovascular MRI from August 2011 to October 2017. The authors also enrolled 100 age- and sex-matched healthy participants to form a comparison group. Trabeculae were quantified with fractal analysis of cine slices to estimate the fractal dimension (FD). Participants with HCM were divided into normal and high FD groups according to the upper limit of normal reference value from the healthy group. The primary end point was defined as all-cause mortality and aborted sudden cardiac death. The secondary end point was the composite of the primary end point and readmission to the hospital owing to heart failure. Internal validation was performed using the bootstrapping method.

Results: A total of 378 participants with HCM (median age, 50 years; age range, 40–61 years; 207 men) and 100 healthy participants (median age, 46 years; age range, 36–59 years; 55 women) were included in this study. During the median follow-up of 33 months ± 18 (standard deviation), the increased maximal apical FD (≥1.325) had a higher risk of the primary and secondary end points than those with a normal FD (<1.325) (P = .01 and P = .04, respectively). Furthermore, Cox analysis revealed that left ventricular maximal apical FD (hazard ratio range, 1.001–1.008; all P < .05) provided significant prognostic value to predict the primary and secondary end points after adjustment for the European Society of Cardiology predictors and late gadolinium enhancement. Internal validation showed that left ventricular maximal apical FD retained a good performance in predicting the primary end points with an area under the curve of 0.70 ± 0.03.

Conclusion: Left ventricular apical fractal dimension, which reflects myocardial trabecular complexity, was an independent predictor of the primary and secondary end points in patients with hypertrophic cardiomyopathy.

© RSNA, 2020

Online supplemental material is available for this article.

Hypertrophic cardiomyopathy (HCM) is a common diagnosis in clinical practice, with a prevalence of one in 500 in the general adult population (1). The clinical phenotypes and prognosis among individuals with HCM are diverse (2). Therefore, early risk stratification to identify patients with HCM at high risk is vital to offer prevention strategies such as implantable cardioverter defibrillator placement. Previous studies based on clinical features (3), serologic markers (4), and cardiovascular imaging (5)

have found many different prognosticators in patients with HCM. However, accurate risk prediction remains unclear.

Currently, two different models are available to identify patients with HCM who are at high risk of sudden cardiac death—the North American model (6) and the European Society of Cardiology (ESC) model (7,8). The North American model is based on five binary clinical risk factors, the presence of any one being an indication for implantable cardioverter defibrillator placement.

Abbreviations

ESC = European Society of Cardiology, FD = fractal dimension, HCM = hypertrophic cardiomyopathy, IQR = interquartile range, LGE = late gadolinium enhancement, LV = left ventricle, RV = right ventricle

Summary

For patients with hypertrophic cardiomyopathy, left ventricular myocardial trabecular complexity derived from cine cardiovascular MRI was an independent predictor of cardiovascular events.

Key Results

- An increased left ventricular (LV) maximal apical fractal dimension (FD) (≥1.325) was associated with the primary (all-cause mortality and aborted sudden cardiac death) and secondary (primary end points in combination with heart failure readmission) end points in participants with hypertrophic cardiomyopathy.
- LV maximal apical FD was an independent predictor of the primary and secondary end points after adjustment for the European Society of Cardiology predictors and late gadolinium enhancement.

The ESC risk score is now routinely used to assess the risk of sudden cardiac death in patients with HCM and the need for an implantable cardioverter defibrillator (7–10). Recently, the enhanced North American model was proposed, and it demonstrated good performance in identifying patients with HCM who are at high risk; however, the model still requires further external validation before it is employed in clinical applications (11).

Noninvasive cardiovascular imaging methods, such as cardiovascular MRI, have assumed increasing importance in the proper phenotyping and risk classification of patients with HCM. For example, late gadolinium enhancement (LGE)—a marker for myocardial fibrosis—has been extensively studied as a risk variable associated with outcome in patients with HCM (12). In addition, the evaluation of trabecular complexity has been acquired by means of fractal analysis, and the calculated unitless index (fractal dimension [FD]), ranging between 1 and 2, from such analysis can reflect the degree of trabecular space filling and complexity (13). FD was derived from standard cine cardiovascular MRI, without the need for special sequences. A previous study (14) reported that the difference in myocardial trabecular complexity using fractal analysis between patients with HCM and healthy volunteers, as well as the increase in myocardial trabecular complexity, has also been identified in subclinical patients with sarcomere protein mutations. However, the prognostic value of myocardial trabecular complexity in HCM remains unclear. In the present study, we aimed to assess the prognostic value of the indexes of trabecular complexity to determine the risk in a prospective cohort of participants with HCM.

Materials and Methods

Study Population

The prospective study was approved by the institutional ethics committee of West China Hospital of Sichuan University, and written informed consent was obtained from each par-

ticipant. Participants with the HCM phenotype who underwent 3.0-T cardiovascular MRI from August 2011 to October 2017 were prospectively enrolled. A total of 376 of the 378 participants with HCM have been previously reported (15). This previous study evaluated the prognostic value of the biventricular long axis strain, whereas in this study, we include new analyses of survival and explore the prognostic value of left ventricular (LV) trabecular complexity. HCM was diagnosed in accordance with the latest American Heart Association and American College of Cardiology guidelines (Appendix E1 [online]) (6). Participants were included if they met the diagnostic criteria for HCM and underwent cardiovascular MRI. We also enrolled 100 age- and sex-matched healthy participants to form a comparison group within the same timeframe, and a total of 76 of the 100 participants were selected from a previous study (16). The exclusion criteria are shown in Figure 1.

Cardiovascular MRI Scans

Electrocardiographically gated cardiovascular MRI was performed using a 3.0-T scanner (Magnetom Trio Tim; Siemens Healthineers, Erlangen, Germany) with a 32-channel cardiac phased-array receiver coil. Steady-state free precession cine images of the entire LV, from the base to the apex, in consecutive short-axis views were acquired during breath holds. Detailed MRI acquisition protocols are available in Appendix E1 (online).

Cardiovascular MRI Analyses

All functional analyses and LGE quantitation were performed by one radiologist (J.S., with 15 years of experience in MRI) using a commercially available software (QMass, version 8.1; Medis Medical Imaging Systems, Leiden, the Netherlands). The tracing method for ventricular function and mass was consistent with that used in previous studies (15,16). Maximal LV wall thickness was measured on short-axis cine images, and it was defined as the greatest dimension at any site within the LV myocardium. LGE is defined automatically by a myocardial signal intensity of 6 standard deviations from the normal myocardium (15,17).

FD Analysis

Fractal analysis was performed by two readers (J.W. and W.C., both with 4 years of cardiovascular MRI experience), who were blinded to each other's data as well as to any other clinical and MRI information. The analysis was performed, according to previous studies (18,19), using Matlab software (MathWorks, Natick, Mass) with custom-written code (FracAnalyse) that has been made freely available online (20). The endocardium and epicardium were manually delineated at the end-diastolic phase of every LV short-axis slice. Then, the FD values were automatically calculated by the software (Fig 2). The global FD was defined as an average of all FD in all measured slices. The LV stack was split into basal and apical halves, and the maximum and mean FD were calculated from the basal or apical half of the ventricle (Fig 3). The entire analysis process can be divided into four steps: (a) bias-
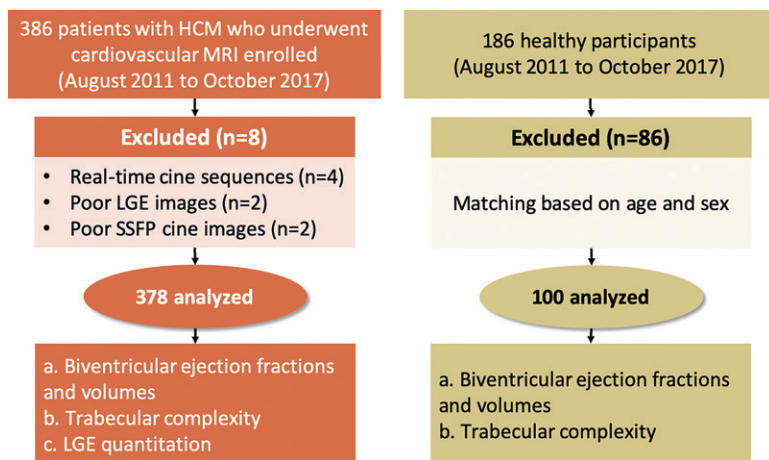
Figure 1: Study inclusion flowchart. HCM = hypertrophic cardiomyopathy, LGE = late gadolinium enhancement, SSFP = steady-state free precession.

field correction using histogram stretching, application of a region-based level-set algorithm, and image binarization to differentiate the LV myocardium and blood pool; *(b)* detection of the endocardial and trabecular borders using a Sobel filter; *(c)* extraction of the endocardial border to calculate the FD with the box-counting method, which is different from other FD equations (13); and *(d)* extraction of the papillary muscles and provision of edges to the final image that then underwent fractal analysis.

Follow-up Data Collection

The clinical follow-up was performed by two cardiologists (Y.L. and F.Y., each with 4 years of experience), who were blinded to the cardiovascular MRI data (Appendix E1 [online]). We documented the primary end points, including cardiovascular death, noncardiovascular death, resuscitated cardiac arrest, and implantable cardioverter defibrillator discharge due to ventricular tachycardia or fibrillation. The secondary end points were composite events comprising the primary end points and readmission to the hospital owing to heart failure.

Statistical Analyses

Statistical analysis was performed using MedCalc software (version 13.0; Ostend, Belgium) and R software (version 4.0.2; The R Project for Statistical Computing, Vienna, Austria). Reproducibility of FD assessment was tested (Appendix E1 [online]). The survival curves were established according to the Kaplan-Meier method, and comparisons were made using the log-rank test. All LV FD values were entered as a continuous variable in univariable and multivariable Cox proportional hazards regression models. Because not all of the LV FD values were completely independent of each other, separate multivariable models were used to test whether each LV FD measure was an independent predictor of the primary and secondary end points, after adjusting for individual ESC risk predictors and percentage of LGE. Bootstrapping was performed to internally validate the prognostic value of apical FD. The area under the curve and calibration were applied to

evaluate the prognostic performance of maximal apical FD (Appendix E1 [online]). In addition, we assessed the effect of LV maximal apical FD adjusted for the ESC risk predictors or score by calculating the improvement of the area under the curve. $P < .05$ was considered indicative of a statistically significant difference.

Results

Demographic and Baseline Clinical Characteristics

We enrolled 386 consecutive participants with HCM. Eight participants were excluded from the study because of poor-quality short-axis cine images (Fig 1), resulting in 378 participants with HCM who were included in the study (median age, 50 years; age range, 40–61 years; 207 men). No significant clinical characteristic differences existed between the eight excluded participants and the rest of the participants with HCM (Table E1 [online]). In addition, 100 healthy participants (median age, 46 years; age range, 36–59 years; 55 women) were enrolled as control participants. The demographic, clinical, and cardiovascular MRI characteristics of all included participants are shown in Table 1. No significant differences existed in age, sex, body surface area, heart rate, LV ejection fraction, and right ventricular (RV) ejection fraction between the two groups. The HCM group had higher systolic blood pressure, larger LV volume, and lower RV volume as compared with the healthy group. The LV mass index was markedly higher in participants with HCM compared with the healthy group (median, 99.0 g/m² ± 36.4 vs 48.7 g/m² ± 12.1; $P < .001$). Additional information for the subgroup of participants with HCM with hypertension is available in Appendix E1 (online).

Comparison of LV FD Characteristics between Participants with HCM and Healthy Participants

Participants with HCM had an elevated LV maximal apical FD compared with healthy participants (mean, 1.345 ± 0.057 vs 1.264 ± 0.044; $P < .001$). Global FD and basal FD were also higher in participants with HCM than in healthy participants (all $P < .001$; Table 1).

Comparison between Participants with HCM with Normal and High LV FD

We set the normal reference of LV FD according to the mean plus 2 standard deviations from the healthy control group (maximal apical FD, 1.352; mean apical FD, 1.270; global FD, 1.256; maximal basal FD, 1.352; mean basal FD, 1.282) and then divided the participants with HCM into high and normal FD groups, using the cut-off value. The two-subgroup comparison is presented in Tables E2 and E3 (online). The high FD group exhibited more severe LV dilation (LV end-diastolic volume index and LV end-systolic volume index; all $P < .05$) and increased LV mass index (all $P < .01$) compared with the normal FD group. In addi-
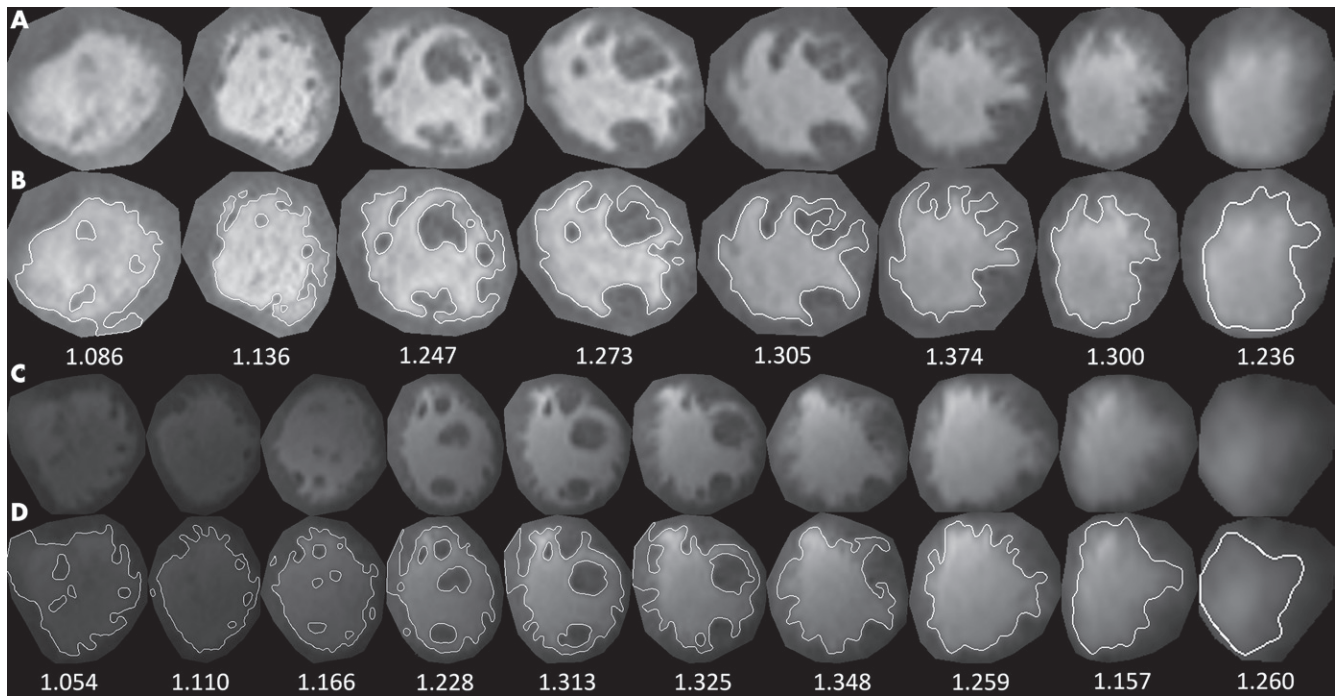
Figure 2: Demonstration of left ventricular fractal dimensions (FDs) in participants with hypertrophic cardiomyopathy (HCM). Examples of short-axis cine and processed fractal pattern from participant with HCM, *A, B,* with primary end point and, *C, D,* without primary end point. FD values were automatically calculated with FracAnalyse software. Global FD was defined as average of all FDs in all measured slices and was 1.245 in *A* and *B* and 1.222 in *C* and *D.* Maximum and mean FDs were calculated from basal or apical half of ventricle (maximal apical FD, 1.374 in *A* and *B* and 1.348 in *C* and *D;* mean apical FD, 1.304 in *A* and *B* and 1.270 in *C* and *D;* maximal basal FD, 1.273 in *A* and *B* and 1.313 in *C* and *D;* mean basal FD, 1.186 in *A* and *B* and 1.174 in *C* and *D).* The number within each image refers to FD value. Primary end point was defined as all-cause mortality and aborted sudden cardiac death (27 events, 7%).
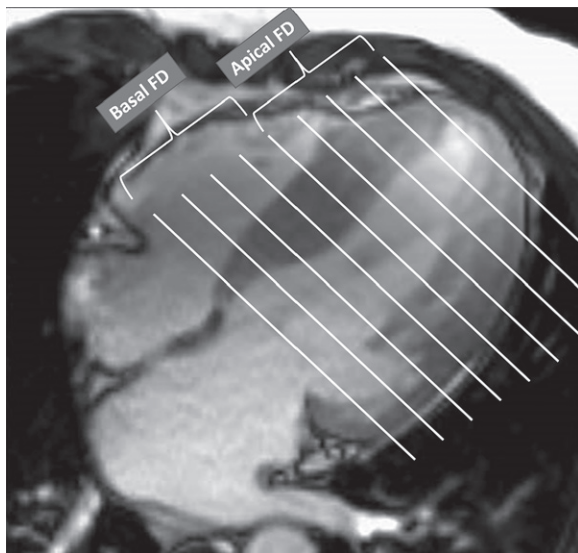

Figure 3: Four-chamber cine image in participant with hypertrophic cardiomyopathy with primary end point illustrates left ventricular (LV) basal and apical fractal dimensions (FDs). LV stack was split into basal and apical halves, and maximum and mean FDs were calculated from basal or apical half of ventricle. Primary end point was defined as all-cause mortality and aborted sudden cardiac death (27 events, 7%).

tion, the HCM subgroup with normal maximal apical FD had lower age compared with the HCM subgroup with high LV maximal apical FD (median age, 49 years, interquartile range [IQR]: 33–59 years vs median age, 51 years, IQR:

43–64 years, respectively; $P = .002$), lower RV ejection fraction (median, 61%, IQR: 55%–66% vs median, 64%, IQR: 57%–68%; $P = .048$), lower LV mass index (median, 84.8 g/m^2, IQR: 66.1–102.1 g/m^2 vs median, 107.5 g/m^2, IQR: 87.8–129.0 g/m^2; $P < .001$), and less LV obstructive HCM (30% vs 52%; $P < .001$) and more apical HCM (31% vs 11%; $P < .001$).

Correlations between LV FD Dimensions and Ventricular Function and Mass Data

In participants with HCM, all LV FD measurements were weakly associated with LV end-diastolic volume index, LV end-systolic volume index, and LV mass index (Table E4 [online]; all $P < .01$). LV global and basal FD were weakly associated with lower LV ejection fraction ($r = -0.16$ to -0.14; $P < .01$). Moreover, global, basal, and maximal apical FDs were weakly associated with maximal LV wall thickness ($r = 0.21$–0.25; $P < .001$). The LV maximal apical FD was weakly correlated with the ESC-derived 5-year HCM risk score ($r = 0.12$; $P = .02$).

Outcomes

During a median follow-up of 33 months $\pm$ 18, 27 of the 378 participants (7%) reached the primary end point, including cardiovascular mortality events in 18 (5%), implantable cardioverter defibrillator discharge events due to ventricular tachycardia or fibrillation in five (1%), resuscitated event from cardiac arrest in one (0.3%), and noncardiovascular deaths in three (1%) (Appendix

Table 1: Demographic, Clinical, and Cardiovascular MRI Phenotypic Characteristics between Participants with HCM and Healthy Participants

Characteristics	Patients with HCM (n = 378)	Healthy Participants (n = 100)	P Value
Age (y)*	50 (40–61)	46 (36–59)	.1
Men	207 (55)	45 (45)	.09
BMI (kg/m²)†	23.8 ± 3.7	22.7 ± 2.7	.005
BSA (m²)‡	1.7 (1.5, 1.8)	1.7 (1.6, 1.8)	.21
SBP (mm Hg)†	123 ± 18	118 ± 11	.006
DBP (mm Hg)†	75 ± 12	80 ± 7	<.001
HR (beats/min)‡	73 (66, 79)	75 (69, 81)	.41
Diabetes mellitus	25 (7)		
Hypertension	91 (24)		
CAD	28 (7)		
Asymptomatic	217 (57)		
Signs of heart failure such as tachypnea	83 (22)		
Chest pain	20 (5)		
Other symptoms (palpitation, dizziness, etc.)	58 (15)		
NYHA functional class			
I	295 (78)		
II	41 (11)		
III	22 (6)		
IV	20 (5)		
Peak LVOT resting gradients (mm Hg)‡§	12 (5, 53)		
Family history of SCD,	50 (13)		
History of syncope	69 (18)		
NSVT	29 (8)		
ESC risk score†	3.3 ± 2.5		
β blocker	259 (69)		
ACEI inhibitors or ARB,	37 (10)		
Spironolactone	39 (10)		
Morphologic characteristics‖			
Reversed curvature	90 (24)		
Midcavity obstruction	99 (26)		
Sigmoid septum	78 (21)		
Apical	85 (22)		
Others	26 (7)		
Obstructive HCM	147 (39)		
Cardiovascular MRI parameters			
LVEF (%)†	62.6 ± 10.2	64.4 ± 6.1	.35
LVEDVi (mL/m²)†	82.2 ± 22.3	73.7 ± 11.9	<.001
LVESVi (mL/m²)†	31.7 ± 17.5	25.7 ± 9.8	.007
RVEF (%)†	60.8 ± 9.4	60.5 ± 5.8	.76
RVEDVi (mL/m²)†	65.4 ± 15.7	69.9 ± 14.0	.02
RVESVi (mL/m²)†	25.7 ± 9.4	27.6 ± 7.2	.03
LV mass index (g/m²)†	99.0 ± 36.4	48.7 ± 12.1	<.001
Max LVT (mm)‡	22.0 (18.0, 25.8)	8.8 (7.9, 9.6)	<.001
LA size (mm)‡	40.0 (35.0, 46.0)	34.0 (29.3, 36.6)	<.001
LGE (%)‡	5.8 (2.1, 12.3)	0	<.001
FDs†			
Global FD	1.267 ± 0.050	1.192 ± 0.032	<.001
Maximal basal FD	1.316 ± 0.064	1.236 ± 0.058	<.001

Table 1 (continues)

Table 1 (continued): Demographic, Clinical, and Cardiovascular MRI Phenotypic Characteristics between Participants with HCM and Healthy Participants

Characteristics	Patients with HCM (*n* = 378)	Healthy Participants (*n* = 100)	*P* Value
Mean basal FD	1.252 ± 0.065	1.182 ± 0.050	<.001
Maximal apical FD	1.345 ± 0.057	1.264 ± 0.044	<.001
Mean apical FD	1.274 ± 0.061	1.192 ± 0.039	<.001

Note.—Except where indicated, data are numbers of patients, with percentages in parentheses. ACEI = angiotensin converting enzyme inhibitor, ARB = angiotensin II receptor blocker, BMI = body mass index, BSA = body surface area, CAD = coronary artery disease, DBP = diastolic blood pressure, ESC = European Society of Cardiology, FD = fractal dimension, HCM = hypertrophic cardiomyopathy, HR = heart rate, LA = left atrium, LGE = late gadolinium enhancement, LV = left ventricle, LVEDVi = LV end-diastolic volume index, LVESVi = LV end-systolic volume index, LVEF = LV ejection fraction, LVOT = LV outflow tract gradient, max LVT = LV maximal wall thickness, NSVT = nonsustained ventricular tachycardia, NYHA = New York Heart Association, RVEF = right ventricular ejection fraction, RVEDVi = right ventricular end-diastolic volume index, RVESVi = right ventricular end-systolic volume index, SBP = systolic blood pressure, SCD = sudden cardiac death.

* Numbers in parentheses are interquartile ranges.

† Numbers are means ± standard deviations.

‡ Numbers are medians, with 25th–75th percentiles in parentheses.

§ Obstructive HCM was defined as LV outflow tract gradient greater than or equal to 30 mm Hg at rest at echocardiography.

‖Morphologic characteristics were defined as follows: *(a)* sigmoid subtype, localized basal septal hypertrophy close to the LV outflow tract; *(b)* reversed curvature, a reverse bulging of the basal anterior and anterior septum toward the LV cavity; *(c)* apical HCM; *(d)* midcavity obstruction; and *(e)* other, that is, did not fit into the preceding four categories.
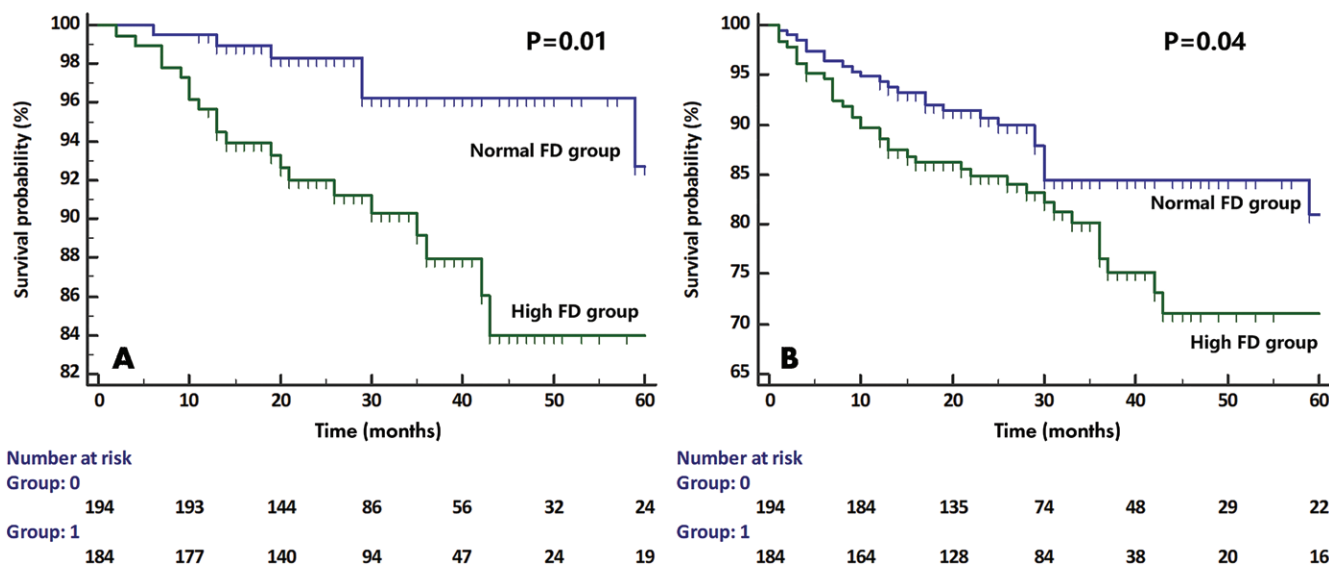

Figure 4: Kaplan-Meier curves for, *A,* primary and, *B,* secondary end points in participants with hypertrophic cardiomyopathy according to the reference value for LV maximal apical fractal dimension (FD) (high FD group ≥1.352 and normal FD group <1.352) from healthy participants. Follow-up of Kaplan-Meier curves is limited to 60 months. Primary end point was defined as all-cause mortality and aborted sudden cardiac death (27 events, 7.1%), and secondary end point was composite of primary end point and readmission to the hospital owing to heart failure (66 events, 18%).

E1 [online]). Additionally, 66 participants (18%) reached the secondary end point with composite adverse events of primary end points or readmission to the hospital owing to heart failure.

Participants with HCM with a maximal apical FD (≥1.352) showed a higher risk of reaching the primary and secondary end points (*P* = .01 and *P* = .04, respectively) (Fig 4). Participants with HCM with a mean apical FD (≥1.270) exhibited a higher rate of reaching secondary end points (*P* = .01) rather than primary end points (*P* = .19). Kaplan-Meier analysis did not indicate any differences in the primary and secondary end points among the other two FD subgroups (all *P* > .05).

Survival Analysis

In a univariable Cox regression analysis, LV FD parameters were significant univariable predictors of the primary end points (all *P* < .05) (Table 2), whereas the global FD (hazard ratio, 1.007, 95% CI: 1.002, 1.012; *P* = .006) and the maximal or mean apical FD (both *P* < .001) were significantly correlated with the secondary end points.

Table 2: Univariable Cox Regression Analysis for the Primary and Secondary End Points in the HCM Cohort

Characteristics	Primary End Point (n = 27)		Secondary End Point (n = 66)	
	Unadjusted Hazard Ratio	P Value	Unadjusted Hazard Ratio	P Value
Sex	1.42 (0.69, 2.95)	.34	1.88 (1.15, 3.07)	.01
ESC risk predictors				
Age (y)	1.04 (1.02, 1.07)	.001	1.05 (1.03, 1.07)	<.001
Peak LVOT resting gradients (mm Hg)	1.00 (0.99, 1.01)	.82	1.008 (1.002, 1.014)	.007
NSVT	2.59 (1.21, 5.57)	.02	2.09 (1.22, 3.58)	.008
Family history of SCD	1.45 (0.55, 3.78)	.47	1.38 (0.72, 2.61)	.36
History of syncope	2.36 (1.10, 5.06)	.03	1.90 (1.12, 3.23)	.03
Left atrium size (mm)	1.07 (1.02, 1.12)	.007	1.09 (1.05, 1.12)	<.001
Max LVT (mm)	1.00 (0.94, 1.07)	.90	1.00 (0.96, 1.04)	.98
Risk factors for adverse events				
Resting peak instantaneous LVOT >30 mm Hg	1.36 (0.66, 2.82)	.41	2.64 (1.62, 4.31)	<.001
Max LVT >30 mm	0.47 (0.06, 3.42)	.46	0.20 (0.03, 1.41)	.11
Percentage of LGE	1.09 (1.05, 1.12)	<.001	1.04 (1.02, 1.06)	<.001
FD (per 1% increase)				
Global FD	1.01 (1.00, 1.02)	.002	1.007 (1.002, 1.012)	.006
Maximal basal FD	1.01 (1.00, 1.01)	.04	1.003 (0.999, 1.007)	.19
Mean basal FD	1.007 (1.001, 1.01)	.03	1.002 (0.998, 1.006)	.38
Maximal apical FD	1.011 (1.005, 1.01)	.001	1.017 (1.006, 1.018)	<.001
Mean apical FD	1.008 (1.003, 1.01)	.006	1.007 (1.004, 1.011)	<.001

Note.—Primary end point is defined as all-cause mortality and aborted sudden cardiac death. Secondary end point is the composite of primary end point and readmission after heart failure hospitalization. Numbers in parentheses are 95% confidence intervals. ESC = European Society of Cardiology, FD = fractal dimension, HCM = hypertrophic cardiomyopathy, LGE = late gadolinium enhancement, LVOT = left ventricular outflow tract gradient, max LVT = left ventricular maximal wall thickness, NSVT = nonsustained ventricular tachycardia, SCD = sudden cardiac death.

In a multivariable Cox analysis, the LV maximal apical FD was the only independent predictor for primary end points (hazard ratio range, 1.001–1.008; all $P < .05$) and secondary end points (hazard ratio range, 1.006–1.007; all $P < .05$), after adjusting for the individual ESC predictors and percentage of LGE, respectively (Table 3).

Performance of New Imaging Risk Predictors
An internal validation, using 100 bootstrapping samples, yielded a mean area under the curve of 0.70 ± 0.03 for LV maximal apical FD to predict the primary end points. With respect to the multivariable Cox models, including maximal apical FD, ESC risk predictors, and LGE, the area under the curve ranged from 0.78 to 0.84. All points on the calibration curve were quite proximate to the 45° line for predicting primary end points at 60 months, which suggested that the LV maximal apical FD had a good performance for stratifying participants with high-risk HCM (Fig E1 [online]).

Furthermore, we fitted a Cox regression model to the ESC risk predictors, and the area under the curve of the ESC risk model for predicting primary end points was 0.72. The ESC risk model was improved by the addition of the LV maximal apical FD (primary end points area under the curve: 0.79; $P < .001$) (Fig E1 [online]).

Reproducibility
We found excellent intra- and interobserver reproducibility (inter- and intraobserver intraclass correlation coefficient, range, 0.79–0.98; inter- and intraobserver coefficient of variation, range, 0.74–2.68). The results are shown in Table E5 (online).

Discussion
In this study, we assessed the prognostic value of left ventricular (LV) myocardial trabecular complexity using fractal analysis in participants with hypertrophic cardiomyopathy (HCM). First, we found that the LV fractal dimension (FD) is significantly higher in participants with HCM than in healthy participants. Second, increased LV maximal apical FD greater than or equal to 1.352 is associated with primary and secondary end points in participants with HCM. Third, in a multivariable Cox analysis, the LV maximal apical FD remains an independent predictor of the primary and secondary end points. Fourth, the addition of LV maximal apical FD yields incremental prognostic value over European Society of Cardiology risk predictors.

Previous studies have reported that fractal analysis is practical, accurate, and reproducible for the identification of patients with hypertrabecular phenotypes (18,21–23). Captur et al (14) reported that all LV FD markers were elevated in patients with HCM, relative to healthy controls (all $P < .001$), consistent with the findings of this study. In addition, Cai et al (23) demonstrated that LV FD was associated with increased cardiac volumes and LV mass and was negatively correlated with diastolic strain rates in healthy volunteers. Moreover, Captur et al (14) also found that LV FD was negatively correlated with LVED volume and stroke volume and was positively correlated with

Table 3: Multivariable Cox Regression Analysis of LV Maximal Apical FD for the Primary and Secondary End Points in the HCM Cohort

Models and Variables	Primary End Point (n = 27)		Secondary End Point (n = 66)	
	Adjusted Hazard Ratio	P Value	Adjusted Hazard Ratio	P Value
Model 1 (n = 378)				
Peak LVOT resting gradients (mm Hg)	1.001 (0.990, 1.012)	.86	1.007 (1.000, 1.013)	.04
Percentage of LGE	1.08 (1.05, 1.11)	<.001	1.04 (1.02, 1.06)	.001
Maximal apical FD	1.007 (1.002, 1.013)	.008	1.006 (1.001, 1.010)	.01
Model 2 (n = 378)				
NSVT	2.07 (0.91, 4.71)	.09	1.69 (0.95, 3.00)	.08
Percentage of LGE	1.07 (1.04, 1.11)	<.001	1.03 (1.01, 1.06)	.008
Maximal apical FD	1.008 (1.002, 1.014)	.006	1.007 (1.003, 1.011)	.001
Model 3 (n = 378)				
Family history of SCD	1.01 (0.36, 2.85)	.99	1.14 (0.57, 2.25)	.72
Percentage of LGE	1.08 (1.05, 1.11)	<.001	1.04 (1.01, 1.06)	.002
Maximal apical FD	1.001 (1.002, 1.013)	.01	1.007 (1.003, 1.011)	.001
Model 4 (n = 378)				
History of syncope	2.12 (0.94, 4.80)	.07	1.61 (0.92, 2.82)	.10
Percentage of LGE	1.08 (1.04, 1.12)	<.001	1.04 (1.01, 1.06)	.002
Maximal apical FD	1.008 (1.002, 1.013)	.009	1.007 (1.003, 1.011)	.002

Note.—Primary end point is defined as all-cause mortality and aborted sudden cardiac death. Secondary end point is the composite of primary end point and readmission to the hospital owing to heart failure. Left ventricular apical maximal fractal dimension is per 1% increase. Due to the sample size and statistical power, we limited each model to three variables (respecting the 1:10 rule). Numbers in parentheses are 95% confidence intervals. FD = fractal dimension, HCM = hypertrophic cardiomyopathy, LGE = late gadolinium enhancement, LV = left ventricle, LVOT = left ventricular outflow tract gradient, NSVT = nonsustained ventricular tachycardia, SCD = sudden cardiac death.

LV mass index, LV ejection fraction, and LGE in patients with HCM. Consistent with these findings, we found that LV FD was associated with cardiac volume, LV mass, and LV ejection fraction in participants with HCM. Multiple adaptation mechanisms could contribute to increased trabecular complexity in HCM.

Zheng et al (22) confirmed that only maximal apical FD is a robust indicator for identifying LV noncompaction from dilated cardiomyopathy. Captur et al (14) found that excessive LV trabecular complexity, particularly in the apical FD, is one of the preclinical HCM phenotypes. Moreover, Dawes et al (18) reported that RV apical FD had the strongest association with survival in pulmonary arterial hypertension. Consistent with these previous studies, only apical FD was found to have prognostic value in the current study, which may be because many patients have no trabeculae at the basal myocardium, and the distal ventricular closing to the apical endocardium is more prone to developmental arrest of the compaction process (24,25) and was related to HCM subtype.

Previous studies have found that the degree of trabeculation influences ventricular mechanics (22,26,27). Captur et al (21) reported that LV maximal apical FD remained significantly higher in hypertension or LV hypertrophy after adjustment for LV mass and hypertension respectively, which indicated that LV hypertrophy may alter the fractal complexity of the LV independent of other parameters. However, it is still unclear whether the normal myocardium transforms into a trabecular meshwork due to ventricular remodeling or whether it is as an adaptive response

to maintain contractile efficiency in HCM (28,29). A previous study has indicated that genetic and environmental factors (30) may influence trabecular formation in patients with HCM. We found that trabecular complexity may provide valuable prognostic information by means of fractal analysis. However, the detailed cause and mechanism of trabecular formation in patients with HCM remain unknown, and further research is needed.

Alashi et al (31) included 2472 patients with obstructive HCM who underwent septal myectomy and reported that 18% of patients were mischaracterized as having HCM, which suggested that some patients with the HCM phenotype may be misdiagnosed according to current diagnostic criteria. Captur et al (14) reported that increased LV apical FDs were detected in sarcomere gene mutation carriers without LV hypertrophy, as compared with healthy volunteers; thus, we may explore whether FD could be a new imaging marker to differentiate diseases mimicking HCM from HCM. Previous studies have demonstrated that it is possible to overdiagnose trabecular complexity according to the current diagnostic criteria of LV noncompaction (32,33). Therefore, there was a need to review the current diagnostic approaches of LV noncompaction. Further research is needed to explore whether fractal analysis could be considered as a new technique to precisely identify LV noncompaction (22).

Our study had several limitations. First, our study was conducted in a relatively low-risk HCM cohort (Appendix E1 [online]) and was a single-center study from China. Additional studies from multiple centers are needed. Second, the peak LV outflow gradient was measured only at rest at echocardiography

and might be underestimated. Third, we used the composite outcome of all-cause mortality and aborted sudden cardiac death rather than cardiovascular mortality as the primary end points. Moreover, our study had a modest sample size, rendering it important to externally validate the findings.

In conclusion, left ventricular fractal dimensions measured with fractal analysis is a readily available and robust parameter reflecting myocardial trabecular complexity. The left ventricular apical fractal dimensions have independent prognostic value for all-cause mortality and composite events, and they provide incremental prognostic value to the European Society of Cardiology predictors in patients with hypertrophic cardiomyopathy.

References

1. Maron BJ, Gardin JM, Flack JM, Gidding SS, Kurosaki TT, Bild DE. Prevalence of hypertrophic cardiomyopathy in a general population of young adults. Echocardiographic analysis of 4111 subjects in the CARDIA Study. Coronary Artery Risk Development in (Young) Adults. Circulation 1995;92(4):785–789.

2. Wang J, Wan K, Sun J, et al. Phenotypic diversity identified by cardiac magnetic resonance in a large hypertrophic cardiomyopathy family with a single MYH7 mutation. Sci Rep 2018;8(1):973.

3. Geske JB, Ong KC, Siontis KC, et al. Women with hypertrophic cardiomyopathy have worse survival. Eur Heart J 2017;38(46):3434–3440.

4. Geske JB, McKie PM, Ommen SR, Sorajja P. B-type natriuretic peptide and survival in hypertrophic cardiomyopathy. J Am Coll Cardiol 2013;61(24):2456–2460.

5. Tower-Rader A, Mohananey D, To A, Lever HM, Popovic ZB, Desai MY. Prognostic Value of Global Longitudinal Strain in Hypertrophic Cardiomyopathy: A Systematic Review of Existing Literature. JACC Cardiovasc Imaging 2019;12(10):1930–1942.

6. Gersh BJ, Maron BJ, Bonow RO, et al. 2011 ACCF/AHA guideline for the diagnosis and treatment of hypertrophic cardiomyopathy: executive summary: a report of the American College of Cardiology Foundation/American Heart Association Task Force on Practice Guidelines. J Am Coll Cardiol 2011;58(25):2703–2738.

7. O'Mahony C, Jichi F, Pavlou M, et al. A novel clinical risk prediction model for sudden cardiac death in hypertrophic cardiomyopathy (HCM risk-SCD). Eur Heart J 2014;35(30):2010–2020.

8. Authors/Task Force members; Elliott PM, Anastasakis A, et al. 2014 ESC Guidelines on diagnosis and management of hypertrophic cardiomyopathy: the Task Force for the Diagnosis and Management of Hypertrophic Cardiomyopathy of the European Society of Cardiology (ESC). Eur Heart J 2014;35(39):2733–2779.

9. O'Mahony C, Jichi F, Ommen SR, et al. International external validation study of the 2014 European society of cardiology guidelines on sudden cardiac death prevention in hypertrophic cardiomyopathy (EVIDENCE-HCM). Circulation 2018;137(10):1015–1023.

10. Liebregts M, Faber L, Jensen MK, et al. Validation of the HCM Risk-SCD model in patients with hypertrophic cardiomyopathy following alcohol septal ablation. Europace. 2018;20(12):198–203.

11. Maron MS, Rowin EJ, Wessler BS, et al. Enhanced American College of Cardiology/American Heart Association strategy for Prevention of Sudden Cardiac Death in High-Risk Patients With Hypertrophic Cardiomyopathy. JAMA Cardiol 2019;4(7):644–657.

12. Weng Z, Yao J, Chan RH, et al. Prognostic Value of LGE-CMR in HCM: A Meta-Analysis. JACC Cardiovasc Imaging 2016;9(12):1392–1402.

13. Captur G, Muthurangu V, Cook C, et al. Quantification of left ventricular trabeculae using fractal analysis. J Cardiovasc Magn Reson 2013;15(1):36.

14. Captur G, Lopes LR, Patel V, et al. Abnormal cardiac formation in hypertrophic cardiomyopathy: fractal analysis of trabeculae and preclinical gene expression. Circ Cardiovasc Genet 2014;7(3):241–248.

15. Yang F, Wang J, Li Y, et al. The prognostic value of biventricular long axis strain using standard cardiovascular magnetic resonance imaging in patients with hypertrophic cardiomyopathy. Int J Cardiol 2019;294:43–49.

16. Li W, Wan K, Han Y, et al. Reference value of left and right atrial size and phasic function by SSFP CMR at 3.0 T in healthy Chinese adults. Sci Rep 2017;7(1):3196.

17. Harrigan CJ, Peters DC, Gibson CM, et al. Hypertrophic cardiomyopathy: quantification of late gadolinium enhancement with contrast-enhanced cardiovascular MR imaging. Radiology 2011;258(1):128–133.

18. Dawes TJW, Cai J, Quinlan M, et al. Fractal Analysis of Right Ventricular Trabeculae in Pulmonary Hypertension. Radiology 2018;288(2):386–395.

19. Captur G, Radenkovic D, Li C, et al. Community delivery of semiautomated fractal analysis tool in cardiac mr for trabecular phenotyping. J Magn Reson Imaging 2017;46(4):1082–1088.

20. Cai J. UK-Digital-Heart-Project/fracAnalyse: fracAnalyse v1.2. 2017.

21. Captur G, Zemrak F, Muthurangu V, et al. Fractal Analysis of Myocardial Trabeculations in 2547 Study Participants: Multi-Ethnic Study of Atherosclerosis. Radiology 2015;277(3):707–715.

22. Zheng T, Ma X, Li S, et al. Value of Cardiac Magnetic Resonance Fractal Analysis Combined With Myocardial Strain in Discriminating Isolated Left Ventricular Noncompaction and Dilated Cardiomyopathy. J Magn Reson Imaging 2019;50(1):153–163.

23. Cai J, Bryant JA, Le TT, et al. Fractal analysis of left ventricular trabeculations is associated with impaired myocardial deformation in healthy Chinese. J Cardiovasc Magn Reson 2017;19(1):102.

24. Mohun TJ, Weninger WJ. Imaging heart development using high-resolution episcopic microscopy. Curr Opin Genet Dev 2011;21(5):573–578.

25. Eidem BW. Noninvasive evaluation of left ventricular noncompaction: what's new in 2009? Pediatr Cardiol 2009;30(5):682–689.

26. Biagini E, Ragni L, Ferlito M, et al. Different types of cardiomyopathy associated with isolated ventricular noncompaction. Am J Cardiol 2006;98(6):821–824.

27. Kawel-Boehm N, McClelland RL, Zemrak F, et al. Hypertrabeculated left ventricular myocardium in relationship to myocardial function and fibrosis: the multi-ethnic study of atherosclerosis. Radiology 2017;284(3):667–675.

28. Alsaileek AA, Syed I, Seward JB, Julsrud P. Myocardial fibrosis of left ventricle: magnetic resonance imaging in noncompaction. J Magn Reson Imaging 2008;27(3):621–624.

29. Cheng H, Zhao S, Jiang S, et al. Comparison of cardiac magnetic resonance imaging features of isolated left ventricular non-compaction in adults versus dilated cardiomyopathy in adults. Clin Radiol 2011;66(9):853–860.

30. Olivotto I, Girolami F, Nistri S, et al. The many faces of hypertrophic cardiomyopathy: from developmental biology to clinical practice. J Cardiovasc Transl Res 2009;2(4):349–367.

31. Alashi A, Desai RM, Khullar T, et al. Different Histopathologic Diagnoses in Patients With Clinically Diagnosed Hypertrophic Cardiomyopathy After Surgical Myectomy. Circulation 2019;140(4):344–346.

32. Ivanov A, Dabiesingh DS, Bhumireddy GP, et al. Prevalence and Prognostic Significance of Left Ventricular Noncompaction in Patients Referred for Cardiac Magnetic Resonance Imaging. Circ Cardiovasc Imaging 2017;10(9):e006174.

33. Femia G, Semsarian C, Richmond D, et al. Abstract 14391: Assessing the Accuracy of the Petersen Criteria for Left Ventricular Non-Compaction with a Novel Thresholding Technique: Long Term Clinical Follow Up. Circulation 2019;140(Suppl_1):A14391.